

HT2013-17146

TRANSIENT INTERNAL FORCED CONVECTION UNDER STEP WALL HEAT FLUX CONDITION**M. Fakoor-Pakdaman**PhD Candidate,
mfakoorp@sfu.ca**Majid Bahrami**Associate Professor,
mbahrami@sfu.ca

Laboratory for Alternative Energy Conversion (LAEC)
Mechatronic Systems Engineering,
School of Engineering Science,
Simon Fraser University,
Surrey, BC, Canada V3T 0A3

ABSTRACT

A new closed-form analytical model is developed to predict transient laminar forced convection inside a circular tube following a time-wise step change in the wall heat flux. The proposed all-time model is based on a blending of two asymptotes; i) short-time asymptote: transient pure conduction in an infinite cylinder and ii) long-time asymptote: steady-state convective heat transfer inside a circular duct. Different fluid velocity profiles are taken into consideration and the model covers: i) Slug Flow (SF); ii) Hydrodynamically Fully Developed Flow (HFDF); and iii) Simultaneously Developing Flow (SDF) conditions. The present model is developed for the entire range of the Fourier and Prandtl numbers. As such, short- and long-time asymptotes for the fluid bulk temperature are obtained. The Nusselt number is defined based on the local temperature difference between the tube wall temperature and the fluid bulk temperature. It is shown that irrespective of the velocity profile, at the initial times the Nusselt number is only a function of time. However, at the steady state condition it depends solely upon the axial location. In addition, during the transient period, the Nusselt number is much higher than that of the long-time response. We also performed an independent numerical simulation using COMSOL Multiphysics to validate the present analytical model. The comparison between the numerical and the present analytical model shows good agreement; a maximum relative difference less than 9.1%.

1. INTRODUCTION

Developing an in depth knowledge of transient heat transfer has drawn significant attention recently with the emergence of sustainable energy applications. In most cases, considerable thermal transients are arising from unsteadiness and dynamic operating conditions in the characteristics of heat

transfer equipment. Generally, processes such as start-up, shut-down, power surge, and pump/fan failure impose such transients [1–4].

The origin of thermal transient in sustainable energy applications includes variable thermal loads of: i) thermal solar panels, commonly used in Thermal Energy Storage (TES) systems; ii) power electronics of solar/wind/tidal energy conversion systems; iii) power electronics and electric motor of Hybrid Electric Vehicles (HEV), Electric Vehicles (EV), and Fuel Cell Vehicles (FCV).

One of the major issues facing renewable energy systems is the inherent intermittence subjected to daily variation, seasonal variation, and weather conditions. As such, the power electronics of the sustainable energy conversion systems and TES systems associated with the thermal solar panels undergo dynamically varying thermal loads. Thus, these systems operate periodically with time and never attain a steady-state condition. Furthermore, the hybrid powertrain and power electronics electric motors (PEEM) of the emerging technology of HEVs, EVs, and FCVs endure dynamic thermal loads as a direct result of driving cycles and environmental conditions. Conventionally, cooling systems are designed based on a nominal steady-state “worst” case scenario, which may not properly represent the thermal behavior of various applications or duty cycles. In-depth knowledge of the instantaneous thermal characteristics of thermal components will provide the platform needed to design and develop new efficient and compact heat exchangers to enhance the overall efficiency and reliability of TES, sustainable energy conversion systems, and PEEM; which in case of the HEV/EV/FCV leads to improved vehicle efficiency and fuel consumption, and reducing weight and emission [5–12].

In all the above-mentioned applications, transient heat transfer occurs inside a component, heat exchanger or a heatsink under arbitrary time-dependent heat flux. This can be represented by unsteady forced-convective tube flow. As such, we have conducted a series of studies to find the transient thermal response of the tube flow under arbitrary time-dependent heat flux. The first step to address the transient heat transfer under dynamically varying heat flux is to solve the governing equations for a time-wise step heat flux which is the case in this paper. In our subsequent papers, we will consider the fluid flow response under dynamically varying heat flux by applying a superposition technique to the results of this paper.

1.1. PERTINENT LITERATURE

A number of studies were conducted on transient forced convection caused by time-wise variations of tube wall temperature or heat flux. Sparrow and Siegel [13] investigated transient heat transfer in the fully developed laminar flow in circular tubes. Siegel and Sparrow [14] performed an analysis for transient laminar heat transfer in the thermal entrance region of a flat duct whose bounding surfaces were subjected to an arbitrary time variation of temperature or heat flux. Siegel [15] studied the laminar slug flow inside parallel plates and circular tubes following a step change in heat flux and tube wall temperature. Improvements on the above solutions were made by Siegel [16] for laminar flow. An integrated form of the energy equation was solved by the method of characteristics. A smooth transition was noted between the transient and steady-state conditions. Hudson and Bankoff [17] performed an analytical study to find an asymptotic solution for unsteady Graetz problem under a stepwise wall temperature. A series solution was presented to find the temperature distribution inside the fluid and the wall heat flux. Lin and Shih [18] applied the instant-local similarity approach to study transients for forced convection inside circular tubes and parallel plates. Cotta and Ozisik [19] analyzed transient laminar forced convection inside parallel plates and circular ducts under stepwise variations of wall temperature. Most of the pertinent papers on transient forced convection under a step heat flux are analytical-based; a summary of the literature is presented in Table 1. Our literature review indicates:

- There is no compact all-time model to predict the fluid flow response under a step heat flux.
- There is no compact model to predict the steady-state heat transfer of slug flow condition.
- The existing models are in form of complex algebraic expressions and series solutions; a large number of terms are necessary to find the accurate results.
- There is no study on the transient forced convection of tube flow with developing velocity profile i.e. Simultaneously Developing Flow (SDF).

In the present study, a compact analytical model is proposed to predict the asymptotic fluid bulk temperature inside a circular tube. Different velocity profiles are taken into consideration and an asymptotic approach is adopted to develop

a closed-form all-time model for the Nusselt number that covers both short-time and steady-state asymptotes. The present all-time model predicts the Nusselt number for the entire range of the Fourier and Prandtl numbers. In most existing studies [13–18], the transient thermal behavior of a system is determined based on the dimensionless wall heat flux, \dot{Q} , considering the difference between the local tube wall and the initial fluid temperature. In the present study, we define the all-time Nusselt number based on the local temperature difference between the tube wall and the fluid bulk temperature at each axial location. We are of the opinion that our definition has a better physical meaning.

To develop the present analytical model the fluid flow response for a step heat flux is taken into account [15]. Various hydrodynamic conditions are considered including i) Slug Flow (SF); ii) Simultaneously Developing Flow (SDF); and iii) Hydrodynamically Fully Developed Flow (HFDF). Short- and long-time asymptotes are developed to determine the Nusselt number and the fluid bulk temperature for the aforementioned cases. The short-time asymptote is corresponding to transient pure conduction inside an infinite cylinder, whereas the long-time asymptote is attributed to the steady-state forced convection inside a circular tube. Consequently, the present compact all-time model is developed based on the blending of the obtained asymptotes. The present compact model covers the entire range of the Fourier and the Prandtl numbers.

2. PROBLEM STATEMENT

Laminar fluid flow inside a circular tube is considered to investigate the transient forced convective tube flows following a step change in the wall heat flux. Figure 1 shows a circular tube of diameter \varnothing which is thermally insulated in the first sub-region, $x \leq 0$, and is heated in the second sub-region $x > 0$. The tube and fluid are assumed to be initially isothermal at temperature T_0 . The wall at the second sub-region is given an instantaneous step in heat flux, $q''(t)$, which is maintained constant thereafter. It is also assumed that the entering fluid temperature and the first sub-region are maintained at T_0 throughout the heating period. The second sub-region may be long enough so that the fluid flow can reach thermally fully developed condition along this section, see Fig. 1. Two extreme conditions are taken into consideration for the inlet velocity profile; this will cover the full range of velocity distribution. As such, Slug Flow (SF) and Hydrodynamically Fully Developed Flow (HFDF) conditions are assumed for the inlet velocity profile of the heated section. The assumed inlet velocity profiles are illustrated in Fig. 2a, b. In addition, to model a more realistic tube flow, Simultaneously Developing Flow (SDF) or the combined entrance region is also considered. In this case, both velocity and temperature profiles are being developed. In fact SDF condition can model the actual thermal and hydrodynamic behavior of the fluids with finite Prandtl numbers [20].

Table 1: Summary of the existing analytical models for unsteady, internal convective heat transfer

Author	Boundary condition and velocity profile	Geometry	Notes
Sparrow and Siegel [13]	Step wall temperature/ heat flux Fully developed flow	Circular duct	Algebraic expressions for the tube wall temperature/heat flux
Siegel and Sparrow [14]	Step wall temperature/heat flux Fully developed flow	Flat duct	Algebraic expressions for the tube wall temperature/heat flux
Siegel [15]	Step wall temperature/ heat flux Slug flow	Circular/flat duct	Series solutions to find the temperature distribution inside the fluid.
Siegel [16]	Step wall temperature Fully developed flow	Circular duct	Series solutions to find the temperature distribution inside the fluid.
Hudson and Bankoff [17]	Step wall temperature Fully-developed flow	Circular duct	Series solutions to obtain the temperature distribution inside the fluid.
Lin and Shih [18]	Step wall temperature Fully-developed flow	Circular duct	Similarity solution to find the Nusselt number; valid only near the tube entrance.
Cotta and Ozisik [19]	Step wall temperature Fully-developed flow	Circular/flat duct	Similarity solution to find the Nusselt number; a large number of eigenvalues needed to obtain accurate results.

It is intended to determine the evolution of the tube wall temperature, fluid bulk temperature and the Nusselt number as a function of time and space for the entire range of the Fourier number. As such, this study aims to propose easy-to-use compact relationships as all-time models representing the thermal behavior of the fluid flow from transient to steady-state conditions.

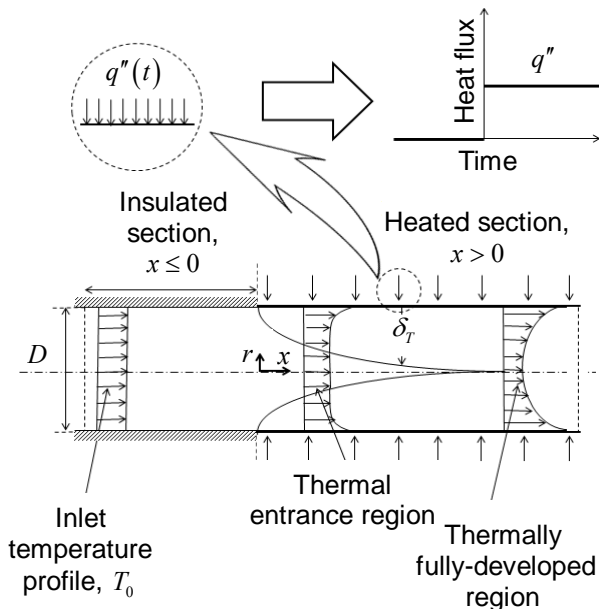


Figure 1. Schematic of the two-region tube and the coordinate system.

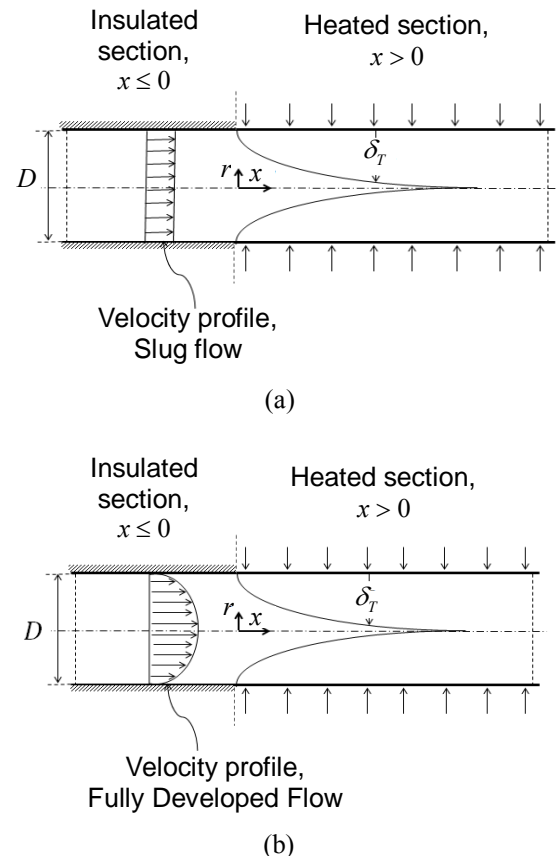


Figure 2. Schematic of the inlet velocity profile for (a) Slug Flow (SF) and (b) Hydrodynamically Fully Developed Flow (HFDF).

2.1. GOVERNING EQUATIONS

The energy equation for a fluid flowing inside a circular duct in this instance is shown by Eq. (1):

$$\frac{\partial T}{\partial t} + u \frac{\partial T}{\partial x} = \alpha \frac{1}{r} \frac{\partial}{\partial r} \left(r \frac{\partial T}{\partial r} \right) \quad (1)$$

It is convenient to non-dimensionalize Eq. (1) by the following dimensionless variables:

$$Fo = \frac{\alpha t}{R^2} \quad X = \frac{4x/D}{\text{Re}_D \cdot \text{Pr}} \quad \theta = \frac{T - T_0}{q'' D / k} \quad \eta = \frac{r}{R}$$

where Fo is the Fourier number and Re_D is the Reynolds number. It should be noted that the mean fluid velocity, u_m , is defined as:

$$u_m = \frac{2}{R^2} \int_0^R u r dr \quad (2)$$

For the case of Slug Flow (SF), the velocity distribution and the energy equation can be written as follows:

$$u(\eta, r) = u_m = \text{const.} \quad (3)$$

$$\frac{\partial \theta}{\partial Fo} + \frac{\partial \theta}{\partial X} = \frac{1}{\eta} \frac{\partial}{\partial \eta} \left(\eta \frac{\partial \theta}{\partial \eta} \right) \quad (4)$$

Similarly for the case of Hydrodynamically Fully Developed Flow (HFDF), the velocity distribution and the energy equation can be written as follows:

$$u(\eta) = 2u_m (1 - \eta^2) \quad (5)$$

$$\frac{\partial \theta}{\partial Fo} + 2(1 - \eta^2) \frac{\partial \theta}{\partial X} = \frac{1}{\eta} \frac{\partial}{\partial \eta} \left(\eta \frac{\partial \theta}{\partial \eta} \right) \quad (6)$$

Consequently, Eqs. (4) and (6) are subjected to the following initial and boundary conditions:

$$\begin{aligned} \theta(X, \eta, 0) &= 0 && \text{Initial condition,} \\ \theta(0, \eta, Fo) &= 0 && \text{Entrance condition,} \\ \left(\frac{\partial \theta}{\partial \eta} \right) \Big|_{\eta=1} &= \frac{1}{2} && \text{Heat flux at the tube wall} \\ &&& \text{for } Fo > 0, \\ \left(\frac{\partial \theta}{\partial \eta} \right) \Big|_{\eta=0} &= 0 && \text{Symmetry at the center} \\ &&& \text{line.} \end{aligned} \quad (7)$$

3. MODEL DEVELOPMENT

A new analytical compact model is developed considering two asymptotes; i) short-time and ii) long-time, steady-state, considering the following assumptions;

- Incompressible flow,
- Constant thermo-physical properties,
- Negligible viscous dissipation,
- Negligible axial heat conduction,
- No thermal energy sources within the fluid,
- Uniform velocity profile along the tube for the Slug Flow (SF) condition,
- Fully developed velocity profile, Poiseuille flow, for the Hydrodynamically Fully Developed Flow (HFDF) condition.
- Developing velocity profile for the Simultaneously Developing Flow (SDF) condition.

3.1. DEFINITION OF THE NUSSELT NUMBER

In this study, the local Nusselt number is defined based on the local difference between the tube-wall and fluid bulk temperatures.

$$Nu_D(x, t) = \frac{q'' D / k}{T_w - T_m} = \frac{1}{\theta_w - \theta_m} \quad (8)$$

Where θ_w and θ_m are the dimensionless wall and fluid bulk temperatures defined as follows.

$$\theta_w = \frac{T_w - T_0}{q'' D / k} \quad \theta_m = \frac{T_m - T_0}{q'' D / k}$$

In addition, T_m is the fluid bulk temperature defined by Eq. (9).

$$T_m = \frac{2}{u_m R^2} \int_0^R u T r dr \quad (9)$$

As indicated by Eq. (9) in order to evaluate the Nusselt number, it is crucial to find an expression to determine the fluid bulk temperature at the transient and steady-state conditions. We perform a one-dimensional transient energy balance on an infinitesimal control volume of the flow, Eq.(10), at an arbitrary location inside the heated part of the tube, $x > 0$, as illustrated in Fig. 3.

$$\begin{aligned} \dot{m} c_p T_m + q'' (\pi D) dx - \\ \left(\dot{m} c_p T_m + \dot{m} c_p \frac{\partial T_m}{\partial x} dx \right) = \rho c_p (\pi D^2 / 4) \frac{\partial T_m}{\partial t} dx \end{aligned} \quad (10)$$

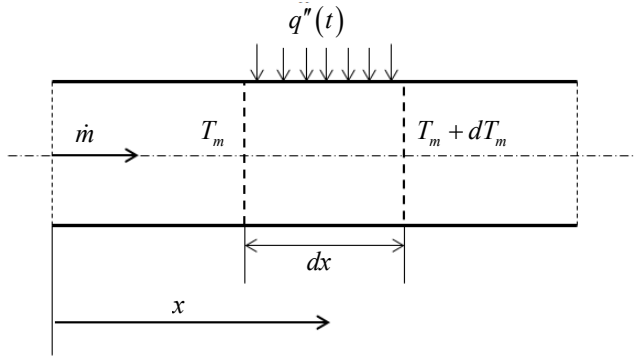


Figure 3. Transient energy balance on a differential control volume of the fluid flow.

The above PDE, Eq. (10), is non-dimensionalized and solved by the method of characteristics. As such, a compact relationship is obtained for the short-time and long-time asymptotic fluid bulk temperatures at a given axial position, Eq. (11).

$$\theta_m = \frac{T_m - T_0}{\frac{q''D}{k}} = \begin{cases} Fo & \text{for } Fo \rightarrow 0 \\ X & \text{for } Fo \rightarrow \infty \end{cases} \quad (11)$$

Therefore, by substituting Eq. (11) into Eq. (8), at a given axial position along the tube, the short-time, and long-time asymptotes of the Nusselt numbers can be defined as Eqs. (12) and (13), respectively.

Short-time asymptote of the Nusselt number, $Fo \rightarrow 0$:

$$Nu_D(t) = \lim_{Fo \rightarrow 0} Nu_D(x, t) = \lim_{Fo \rightarrow 0} \frac{1}{\theta_w - Fo} \quad (12)$$

Long-time asymptote of the Nusselt number, $Fo \rightarrow \infty$:

$$Nu_D(x) = \lim_{Fo \rightarrow \infty} Nu_D(x, t) = \lim_{Fo \rightarrow \infty} \frac{1}{\theta_w - X} \quad (13)$$

The all-time Nusselt number is indicated as $Nu_D(x, t)$, while the short-time and steady-state Nusselt numbers are denoted as $Nu_D(t)$ and $Nu_D(x)$, respectively. Regarding Eqs. (12) and (13), compact correlations can be proposed for the short-time and steady-state asymptotes of the Nusselt number once the dimensionless tube wall temperature is obtained.

3.2. SHORT-TIME ASYMPTOTE, $Fo \rightarrow 0$

The solution to Eq. (4) proceeds as follows: consider a position x in the tube. After heating begins, the fluid which is at the entrance of the channel when the transient began will have travelled a certain distance down the tube. Beyond this distance there will not be any penetration of the entrance fluid which has

been originally outside the tube. Hence, the heat flow in this region will not be affected by the fact that the tube has an entrance. The behavior in this region is then that of a tube of infinite length in both directions, and there is no variation of heat transfer quantities with distance x . Therefore, the fluid at any axial position undergoes the same transient heating process as that at any other axial position, and the effects of heat convection is zero [16]. This indicates that the convective term in the energy equation, Eq. (4), is identically zero. Thus, Eq. (4) will be reduced to a one-dimensional transient heat conduction case at the short-time response. Therefore, the solution of Eq. (4) is the same as that for suddenly applying a uniform heat flux at the surface of an infinite cylinder [15], i.e. Eq. (14).

$$\theta(\eta, Fo) = Fo + \frac{2\eta^2 - 1}{8} - \sum_{n=1}^{\infty} e^{-\beta_n^2 Fo} \frac{J_0(\beta_n \eta)}{\beta_n^2 J_0(\beta_n)} \quad (14)$$

Where $\theta(\eta, Fo)$ is the short-time temperature distribution inside the fluid; β_n are the positive roots of $J_1(\beta) = 0$ and $J_1(\beta)$ are the Bessel functions of the first kind, respectively.

Considering Eq.(14), the short-time dimensionless tube wall temperature and wall heat flux can be written as Eqs. (15) and (16), respectively.

$$\theta_w = \frac{T_w - T_0}{\frac{q''D}{k}} = \theta|_{\eta=1} = Fo + \frac{1}{8} - \sum_{n=1}^{\infty} \frac{e^{-\beta_n^2 Fo}}{\beta_n^2} \quad (15)$$

$$\dot{Q}(t) = \frac{\frac{q''R}{k}}{T_w - T_0} = \frac{1}{2\theta_w} = \frac{1}{2 \left(Fo + \frac{1}{8} - \sum_{n=1}^{\infty} \frac{e^{-\beta_n^2 Fo}}{\beta_n^2} \right)} \quad (16)$$

Incropera *et al.* [21] proposed the following approximate easy-to-use relation for Eq. (15):

$$\theta_w = \left(\sqrt{\frac{\pi}{Fo}} - \frac{\pi}{4} \right)^{-1} \quad (17)$$

For $Fo \leq 0.2$, Eq. (17) can predict the results obtained by the exact solution, Eq.(15), with a maximum relative difference less than 2.1% [21].

Now that the short-time tube wall temperature is obtained, we substitute Eq. (17) into Eqs. (12) and (16), to find the short-time asymptote of the dimensionless wall heat flux and the Nusselt number as follows.

$$\dot{Q}(t) = \lim_{Fo \rightarrow 0} \frac{1}{2\theta_w} = \lim_{Fo \rightarrow 0} 0.5 \left(\sqrt{\frac{\pi}{Fo}} - \frac{\pi}{4} \right) \approx 0.5 \sqrt{\frac{\pi}{Fo}} \quad (18)$$

$$Nu_D(t) = \lim_{Fo \rightarrow 0} \frac{1}{\theta_w - \theta_m} = \lim_{Fo \rightarrow 0} \frac{1}{\frac{1}{\sqrt{\frac{\pi}{Fo} - \frac{\pi}{4}}} - Fo} \approx \sqrt{\frac{\pi}{Fo}} \quad (19)$$

It should be noted that in Eq. (18) as $Fo \rightarrow 0$, the term $\sqrt{\frac{\pi}{Fo}}$ is much higher than $\frac{\pi}{4}$. Therefore, the latter will drop at the initial times. Depicted in Fig. 4 are the variations of the dimensionless wall heat flux, Eqs. (16) and (18), versus the Fourier number for the Slug Flow (SF) condition. It is evident from Fig. 4 that almost 30 terms of the exact series solution, Eq.(16), should be used to obtain accurate results especially for the very small Fourier numbers. This happens since as $Fo \rightarrow 0$ the exponential term in Eq. (16) is quite large compared to the other terms. However, as $Fo \rightarrow \infty$ this term decreases significantly with time and it drops for the large Fo numbers. In addition, there is a good agreement between the short-time asymptote, Eq.(18), and the exact series solution, Eq.(16), especially for the small Fourier numbers, $Fo < 0.1$. The maximum relative difference between the results is less than 9.1% for $Fo < 0.1$ which assures the validity of the developed short-time asymptote.

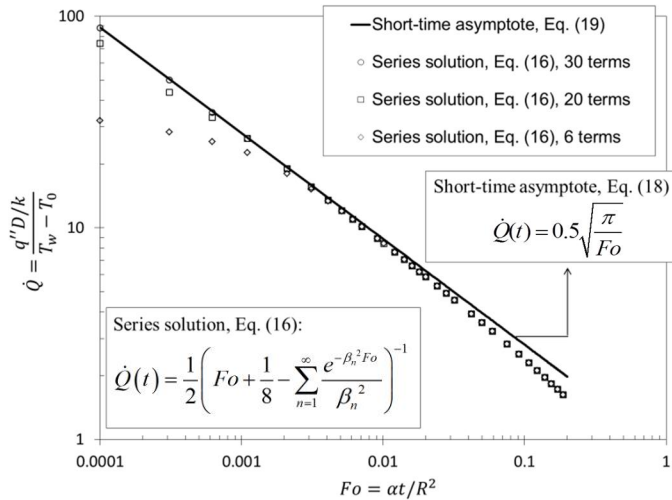


Figure 4. Short-time asymptote, Eq. (18), for the dimensionless heat flux of Slug Flow (SF), Simultaneously Developing Flow (SDF) and Hydrodynamically Fully Developed Flow (HFDF) conditions in comparison with the exact solution , Eq. (16).

In addition, as also mentioned by Sparrow and Siegel [13], the transient response for the case of Poiseuille flow is exactly the same as that of the slug flow condition. In other words, irrespective of the velocity distribution, at initial times the heat transfer process is dominated by pure conduction.

Therefore, Eqs. (18) and (19) can be used as the short-time asymptotes for SF, HFDF, and SDF conditions. As previously mentioned, the short-time asymptote, $Nu_D(t)$, is only a function of time, and it can be used to find the Nusselt number at any axial position along the tube for small Fourier numbers, $Fo \rightarrow 0$.

3.3. LONG-TIME ASYMPTOTE, $Fo \rightarrow \infty$

The long time asymptote, $Fo \rightarrow \infty$, for the tube flow is corresponding to the steady-state internal forced-convection heat transfer. In this case the transient term in Eq. (1) is identically zero, and the governing equations reduce to the classical steady Graetz problem.

Although the short-time asymptote was the same for all the conditions considered here, different steady-state asymptotes must be used. In broad terms, due to the presence of the convective term in the steady state form of the energy equation, different solutions are obtained for the considered cases here with different velocity profiles, including: i) Slug Flow (SF); ii) Hydrodynamically Fully Developed Flow (HFDF); and iii) Simultaneously Developing Flow (SDF) conditions. As such, a new compact model is developed in this study to predict the steady-state heat transfer of slug flow inside a circular tube. However for the other cases i. e. HFDF and SDF, compact relationships developed in the literature are used.

3.3.1. Slug Flow (SF) condition

Equation (4) is the dimensionless energy equation for the Slug Flow (SF) condition. The steady-state solution to this equation is given below [15].

$$\theta = X + \frac{2\eta^2 - 1}{8} - \sum_{n=1}^{\infty} e^{-\beta_n^2 X} \frac{J_0(\beta_n \eta)}{\beta_n^2 J_0(\beta_n)} \quad \text{for } Fo \rightarrow \infty \quad (20)$$

where β_n are the positive roots of $J_1(\beta) = 0$ and $J_1(\beta)$ are the Bessel functions of the first kind, respectively.

By evaluating the fluid temperature at the tube wall, Eq.(20), the steady-state tube wall temperature is obtained.

$$\theta_w = \theta|_{\eta=1} = X + \frac{1}{8} - \sum_{n=1}^{\infty} \frac{e^{-\beta_n^2 X}}{\beta_n^2} \quad (21)$$

By substituting Eq. (21) into Eq.(13), the steady-state Nusselt number for the Slug Flow (SF) can be obtained.

$$Nu_D(x) = \lim_{Fo \rightarrow \infty} \frac{1}{\theta_w - X} = \frac{1}{\frac{1}{8} - \sum_{n=1}^{\infty} \frac{e^{-\beta_n^2 X}}{\beta_n^2}} \quad (22)$$

Incropera *et al.* [21] proposed compact correlations to predict the series solution represented by Eq. (21) as follows.

$$\theta_w = \begin{cases} \left(\sqrt{\frac{\pi}{X}} - \frac{\pi}{4} \right)^{-1} & \text{for } X < 0.2 \\ X + \frac{1}{8} & \text{for } X \geq 0.2 \end{cases} \quad (23)$$

Substituting Eqs. (23) into Eq. (13), the steady-state asymptotes for the Nusselt number for the Slug Flow (SF) is obtained:

$$Nu_D(x) = \begin{cases} \left[\left(\sqrt{\frac{\pi}{X}} - \frac{\pi}{4} \right)^{-1} - X \right]^{-1} & \text{for } X < 0.2 \quad (24a) \\ 8 & \text{for } X \geq 0.2 \quad (24b) \end{cases}$$

Figure 5 illustrates the variations of the steady-state Nusselt number versus the axial position.

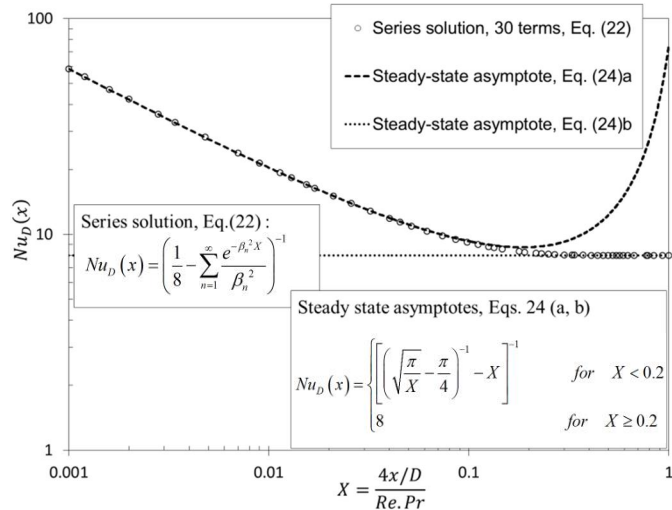


Figure 5. Obtained steady-state asymptotic Nusselt numbers, Eq. 24(a, b), for Slug Flow (SF) condition, and comparison with the exact solution, Eq. (22).

As shown in Fig. 5, a good agreement is found between Eq. (24)a and the exact results for small axial positions, $X < 0.2$. It should be noted that for the Slug Flow (SF) condition, the energy equation is symmetric with respect to the Fourier number and axial position. Hence, again up to 30 terms are necessary to obtain accurate results for small axial positions, $X < 0.2$. Moreover, when $X \geq 0.2$, Eq. (24)b can satisfactorily predict the exact results. The maximum discrepancy between the exact results, Eq.(22), and the ones predicted by the developed long-time asymptote, Eq. (24)b, is less than 2.1% as stated in [21].

3.3.2. Hydrodynamically Fully Developed Flow (HFDF)

Churchill and Ozoe [24] proposed a compact correlation to obtain the Nusselt number for the entire range of axial position.

$$\frac{Nu_D(x)+1}{5.364} = \left[1 + \left(\frac{55}{\pi} X \right)^{-10/9} \right]^{3/10} \quad (25)$$

Therefore, Eq. (25) is considered as the steady-state asymptote for the Hydrodynamically Fully Developed Flow (HFDF) condition.

3.3.3. Simultaneously Developing Flow (SDF)

The most realistic model of the tube flow problem consists of solving Eq. (1) with a developing velocity profile. A closed-form expression that covers both the entrance and fully developed regions was developed by Churchill and Ozoe [24].

$$\frac{Nu_D(x)}{4.364 \left[1 + \left(\frac{\pi}{29.6X} \right)^2 \right]^{1/6}} = \left\{ 1 + \left[\frac{\frac{\pi}{19.04X}}{\left[1 + \left(\frac{Pr}{0.0207} \right)^{2/3} \right]^{1/2} \left[1 + \left(\frac{\pi}{55X} \right)^2 \right]^{1/3}} \right]^{3/2} \right\}^{1/3} \quad (26)$$

Therefore, Eq. (26) will be considered as the steady-state asymptote for the Simultaneously Developing Flow (SDF) condition.

3.4. NUMERICAL SIMULATION

In Sections 3.2 and 3.3, we obtained the short-time and the long-time, steady-state, asymptotes of the Nusselt number for different hydrodynamic conditions. In this section, we investigate the thermal behavior of the flow under transition condition numerically. The transition period for each axial position is defined as the time span in which that position reaches the steady-state condition. In addition, the proposed analytical solutions and the asymptotes presented in the previous sections are validated by the present numerical simulation.

COMSOL Multiphysics (version: 4.2a), a commercial FEM code, is used to simulate the thermal behavior of the tube flows, [25]. Stationary solver is used for the laminar flow inside the tube, whereas time dependent solver is selected for the laminar heat transfer inside the fluid. The numerical results are also used to combine the short-time and steady-state asymptotes to develop new general compact relationships. The obtained numerical data are non-dimensionalized, and compared with the analytical results presented in Section 4. The Nusselt number is computed by Eq.(8), while the bulk-fluid temperature is evaluated by Eq.(11). Furthermore, the assumptions stated in Section 0 are used in the numerical

analysis. Grid independence is tested for different cases and the size of computational grids is selected such that the maximum difference in the predicted values for the Nusselt number is less than 2%.

3.5. ALL-TIME MODEL

A new all-time model is proposed in this section using a combination of the short-time and steady-state asymptotes, reported in Sections 3.2 and 3.3, in the following form:

$$Nu_D(x,t) = [Nu_D^n(t) + Nu_D^n(x)]^{\frac{1}{n}} \quad (27)$$

Where $Nu_D(x,t)$ is the all-time Nusselt number, whereas $Nu_D(t)$ and $Nu_D(x)$ are short-time and steady state asymptotes, respectively. This method of combining asymptotic solutions, also known as blending technique, was introduced by Churchill and Usagi [26]. This approach assumes that a smooth transition occurs between the two asymptotes. The parameter n introduced in Eq. (27) may be chosen using a number of methods as discussed by Churchill and Usagi [26]. In this study, the parameter n is chosen as the value which minimizes the root mean square (RMS) difference between the model predictions and the present numerical data.

4. RESULTS AND DISCUSSION

Several new closed-form compact relations are developed for different flow conditions considered here. The obtained results are categorized and described in the following sections.

4.1. SLUG FLOW (SF) CONDITION

The following all-time models are developed to predict the Nusselt number of the Slug Flow (SF) condition over the entire range of the Fourier number.

$$Nu_D(x,t) = \begin{cases} \left\{ \left(\sqrt{\frac{\pi}{Fo}} \right)^{10} + \left[\frac{1}{\left(\sqrt{\frac{\pi}{X} - \frac{\pi}{4}} \right)^{-1} - X} \right]^{10} \right\}^{\frac{1}{10}} & \text{for } X < 0.2 \\ \left[\left(\sqrt{\frac{\pi}{Fo}} \right)^{10} + (8)^{10} \right]^{\frac{1}{10}} & \text{for } X \geq 0.2 \end{cases} \quad (28)$$

Variations of the asymptotic Nusselt numbers versus the Fourier number for the Slug Flow (SF) condition are plotted in Fig. 6 and compared with our numerical data. In addition, the present all-time model for SF condition, Eq.(28), is illustrated in Fig. 7, and compared with numerical and asymptotic results. The agreement between the present all-time model and the numerical data is excellent, the maximum and average relative difference are approximately 6 and 1%, respectively. The following can be concluded from Figs. 6 and 7:

- At the short-time limit, $Fo \rightarrow 0$, heat transfer only occurs via conduction.
- At a given axial position, $X = \frac{4x/D}{Re \cdot Pr}$, Nusselt number values are stabilized at the steady-state condition ($Fo \rightarrow \infty$). Therefore, at initial times the Nusselt number is only a function of time, not the axial location. On the other hand, at the steady-state condition, $Fo \rightarrow \infty$, the Nusselt number is only a function of axial position. Over the transition period, heat transfer is a function of both time and axial position.
- The Nusselt number decreases drastically with time; also reduces with the axial position along the channel.
- Comparing short-time and steady-state asymptotes, it is noteworthy to mention that the heat transfer at initial times is several orders of magnitude higher than that of the larger Fo numbers.

4.2. HYDRODYNAMICALLY FULLY DEVELOPED FLOW (HFDF)

Similarly, the following all-time relationship, Eq.(29), is developed to predict the Nusselt number for the Hydrodynamically Fully Developed Flow (HFDF) condition for the entire range of the Fourier number.

$$Nu_D(x,t) = \left\{ \left(\sqrt{\frac{\pi}{Fo}} \right)^7 + \left\{ 5.364 \left[1 + \left(\frac{55}{\pi} X \right)^{-\frac{10}{9}} \right]^{\frac{3}{10}} - 1 \right\}^7 \right\}^{\frac{1}{7}} \quad (29)$$

It should be noted that the maximum and average relative difference between the numerical data and the all-time model, Eq.(29), are 9 and 1.6%, respectively.

4.3. SIMULTANEOUSLY DEVELOPING FLOW (SDF)

The following all-time compact relation is proposed for the Simultaneously Developing Flow (SDF) condition.

$$Nu_D(x,t) = \left\{ \left(\sqrt{\frac{\pi}{Fo}} \right)^{10} + [Nu_D(x)]^{10} \right\}^{1/10} \quad (30)$$

Where $Nu_D(x)$ is the steady-state asymptote for the SDF condition defined by Eq.(26). The maximum and average relative difference between the values predicted by Eq. (30) and the numerical data are 6 and 1.5%, respectively. The correlations presented in this study are summarized in Table 2.

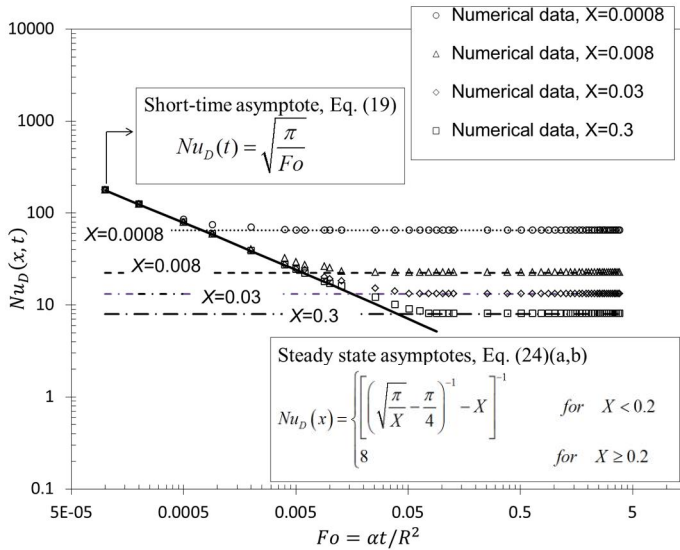


Figure 6. Comparison between the asymptotic, Eq. (19), and numerical Nusselt numbers against the Fourier number for the SF condition.

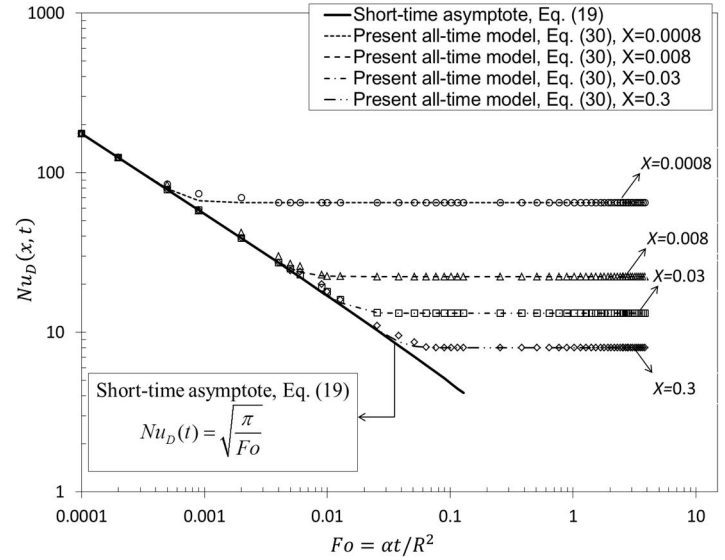


Figure 7. Variations of the Nusselt number predicted by the present all-time model, Eq. (30), versus the Fourier number for SF condition in comparison with the numerical/asymptotic results, Eq. (19).

Table 2. Present all-time model for different cases considered in this study.

Flow condition	All-time model $Nu_D(x,t)$	Steady-state asymptote $Nu_D(x)$
SF	$[Nu_D^{10}(t) + Nu_D^{10}(x)]^{1/10}$	$\begin{cases} \left[\left(\sqrt{\frac{\pi}{X} - \frac{\pi}{4}} \right)^{-1} - X \right]^{-1} & \text{for } X < 0.2 \\ 8 & \text{for } X \geq 0.2 \end{cases}$
HFDF	$[Nu_D^7(t) + Nu_D^7(x)]^{1/7}$	$5.364 \left[1 + \left(\frac{55}{\pi} X \right)^{-10/9} \right]^{3/10} - 1$
SDF	$[Nu_D^{10}(t) + Nu_D^{10}(x)]^{1/10}$	$\left\{ 4.364 \left[1 + \left(\frac{\pi}{29.6X} \right)^2 \right]^{1/6} \right\} \times \left[1 + \left[\frac{\frac{\pi}{19.04X}}{\left[1 + \left(\frac{\text{Pr}}{0.0207} \right)^{2/3} \right]^{1/2} \left[1 + \left(\frac{\pi}{55X} \right)^2 \right]^{1/3}} \right]^{3/2} \right]^{1/3}$

Short-time asymptote: $Nu_D(t) = \sqrt{\frac{\pi}{Fo}}$

5. CONCLUSION

A new compact analytical model is developed to predict the full-range-time forced convection heat transfer inside a

circular tube following a step change in the wall heat flux. The present model is developed using on a blending technique to match the two asymptotes corresponding to transient pure

conduction in an infinite cylinder and the steady-state convection heat transfer inside an iso-heat-flux tube. Slug Flow (SF), Hydrodynamically Fully Developed Flow (HFDF), and Simultaneously Developing Flow (SDF) conditions are taken into account, and several all-time relations are developed to predict the Nusselt number for the entire range of the Fourier and Prandtl numbers.

The highlights of this study are listed below:

- At initial times, $Fo \rightarrow 0$, irrespective of the fluid velocity distribution, the heat transfer occurs only via conduction, and the Nusselt number is only a function of time, $Nu_D(t)$.
- At steady-state condition, $Fo \rightarrow \infty$, the Nusselt number is only a function of axial position, $Nu_D(x)$.
- There is a smooth transition from transient to steady-state condition where the Nusselt number is a function of both time and axial position.
- The Nusselt number at initial times is remarkably higher than that of the steady-state condition.
- The fluid bulk temperature along the channel is only a function of time at initial times, while it stabilizes at each axial position as it reaches the steady-state condition.

The analytical results are successfully validated against the numerical data obtained independently in this study. The maximum relative difference between the analytical model and the numerical data is less than 9.1%.

ACKNOWLEDGEMENT

This work was supported by Automotive Partnership Canada (APC), Grant No. APCPJ 401826-10. The authors would like to thank the support of the industry partner of the project, Future Vehicle Technologies Inc. (British Columbia, Canada).

REFERENCES

- [1] F. Agyenim, N. Hewitt, P. Eames, and M. Smyth, "A review of materials, heat transfer and phase change problem formulation for latent heat thermal energy storage systems (LHTESS)," *Renewable and Sustainable Energy Reviews*, vol. 14, no. 2, pp. 615–628, Feb. 2010.
- [2] M. Hale, "Survey of thermal storage for parabolic trough power plants," *NREL report*, no. September, pp. 1–28, 2000.
- [3] J. B. Garrison and M. E. Webber, "Optimization of an integrated energy storage for a dispatchable wind powered energy system," in *ASME 2012 6th International Conference on Energy Sustainability*, 2012, pp. 1–11.
- [4] J. L. Sawin and E. Martinot, "Renewables Bounced Back in 2010, Finds REN21 Global Report," 2011.
- [5] "http://en.wikipedia.org/wiki/Renewable_energy."
- [6] T. I. TMC Press Release, "Cumulative Sales of TMC Hybrids Top 2 Million Units in Japan," 2012.
- [7] K. Bennion and M. Thornton, "Integrated vehicle thermal management for advanced vehicle propulsion technologies : Integrated Vehicle Thermal Management for Advanced Vehicle Propulsion Technologies," *NREL report*, pp. 1–15, 2010.
- [8] K. J. Kelly, T. Abraham, K. Bennion, D. Bharathan, S. Narumanchi, and M. O. Keefe, "Assessment of thermal control technologies for cooling electric vehicle power electronics," *NREL report*, no. January, 2008.
- [9] T. Kojima, Y. Yamada, and W. Fichtner, "A novel electro-thermal simulation approach of power IGBT modules for automotive traction applications," in *Proceedings of the 16th International Symposium on Power Semiconductor Devices & IC's*, 2004, no. v, pp. 289–292.
- [10] R. W. Johnson, J. L. Evans, P. Jacobsen, J. R. R. Thompson, and M. Christopher, "The changing automotive environment: high-temperature electronics," in *IEEE Transactions on Electronics Packaging Manufacturing*, 2004, vol. 27, no. 3, pp. 164–176.
- [11] M. Marz and A. Schletz, "Power electronics system integration for electric and hybrid vehicles," ... *Power Electronics ...*, pp. 16–18, 2010.
- [12] W.-R. Canders, G. Tareilus, I. Koch, and H. May, "New design and control aspects for electric vehicle drives," in *Proceedings of 14th International Power Electronics and Motion Control Conference EPE-PEMC 2010*, 2010.
- [13] E. M. Sparrow and R. Siegel, "Thermal entrance region of a circular tube under transient heating conditions," in *Third U. S. National Congress of Applied Mechanics*, 1958, pp. 817–826.
- [14] R. Siegel and E. M. Sparrow, "Transient heat transfer for laminar forced convection in the thermal entrance of flat ducts," *Heat Transfer*, vol. 81, pp. 29–36, 1959.
- [15] R. Siegel, "Transient heat transfer for laminar slug flow in ducts," *applied Mechanics*, vol. 81, no. 1, pp. 140–142, 1959.
- [16] R. Siegel, "Heat transfer for laminar flow in ducts with arbitrary time variations in wall temperature," *Applied Mec*, vol. 27, no. 2, pp. 241–249, 1960.
- [17] J. L. Hudson and S. G. Bankoff, "Asymptotic solutions for the unsteady Graetz problem," *Int. J. Heat Mass Transfer*, vol. 7, pp. 1303–1307, 1964.

- [18] H. T. Lin and Y. P. Shih, "Unsteady thermal entrance heat transfer of power-law fluids in pipes and plate slits," *Int. J. Heat Mass Transfer*, vol. 24, pp. 1531–1539, 1981.
- [19] R. M. Cotta and M. N. Ozisik, "Transient forced convection in laminar channel flow with stepwise variations of wall temperature," *Canadian Journal of Chemical Engineering*, vol. 64, no. 5, pp. 734–742, 1986.
- [20] A. Bejan, *Convection heat transfer*, Third. John Wiley & Sons, 2004.
- [21] F. P. Incropera, D. P. Dewitt, T. L. Bergman, and A. S. Lavine, *Introduction to heat transfer*, Fifth. USA: John Wiley & Sons, 2007.
- [22] R. Siegel, E. M. Sparrow, and T. M. Hallman, "Steady laminar heat transfer in a circular tube with prescribed wall heat flux," *Appl. Sci. Res.*, vol. 7, pp. 386–392, 1958.
- [23] R. K. Shah and A. L. London, *Laminar flow forced convection in ducts*. New York: Academic Press, 1978.
- [24] S. W. Churchill and H. Ozoe, "Correlations for laminar forced convection with uniform heating in flow over a plate and in developing and fully developed flow in a tube," *Heat Transfer*, vol. 95, pp. 78–84, 1973.
- [25] "COMSOL Multiphysics Instruction Manual," USA, 2011.
- [26] S. W. Churchill and R. Usagi, "A General Expression for the Correlation of Rates of Transfer and Other Phenomena," *American Institute of Chemical Engineers*, vol. 18, pp. 1121–1128, 1972.